AIAA JOURNAL
Vol. 48, No. 3, March 2010

Vibration Analysis of a Multiple-Layered Viscoelastic Structure Using the Biot Damping Model

Fei Lin* and Mohan D. Rao†
Michigan Technological University, Houghton, Michigan 49931

DOI: 10.2514/1.44339

The viscoelastic damping treatment is a very popular method for attenuating vibration and noise problems. It provides the designer much flexibility in adjusting the system damping to eliminate resonances in the structures. A survey of the previous research on material damping models found inadequacies in developing the numerical models of multiple-layer constrained layers and the introduction of the combination of different viscoelastic damping materials through advanced frequency domain damping models. In this paper, a detailed numerical analysis and design of a multiple-layer constrained damping structure using the Biot damping model are presented to investigate the vibration performance. The nonlinear curve fitting of the complex shear modulus and the transient response solution of the numerical viscoelastic damping structure are also discussed. By the proposed approach, the simple beam problem that is presented can be easily extended to the industrial problem with arbitrary geometries and boundary conditions. The validation of this numerical approach is proven by comparison with the previous closed-form results.

Nomenclature

$\mathbf{A}$, $\mathbf{B}$	=	coefficient matrix of state equation
$\mathbf{D}$	=	damping matrix
$\mathbf{E}$	=	Young's Modulus
$\mathbf{f}$	=	force vector
$\mathbf{G}$	=	shear modulus
G^{∞}, $\{a_k, b_k\}$	=	Biot constants
$\mathbf{h}$	=	thickness of layer
$\boldsymbol{K_e}$, $\boldsymbol{K_v}$	=	elastic stiffness and viscous stiffness matrices
l	=	length of beam
$\mathbf{M}$	=	mass matrix
$\mathbf{m}$, $\mathbf{n}$	=	number of minioscillators for first and second types of viscoelastic materials
$\mathbf{N}$	=	number of degrees of freedom
$\mathbf{N_e}$, $\mathbf{N_f}$	=	finite element shape function of longitudinal and transverse deflections
$\mathbf{s}$	=	Laplace variable
$\mathbf{t}$	=	time
$\mathbf{x}$	=	displacement vector
$\mathbf{z}$	=	dissipation coordinate vector
$\boldsymbol{\lambda}$	=	eigenvalue matrix
ρ	=	density of material
$\boldsymbol{\Phi}$	=	eigenvector matrix

I. Introduction

VIBRATION and noise issues are essential to the improvement of performance and operational perception in the most advanced engineering products and systems subjected to dynamic and shock loadings. Passive and active structural damping can attenuate the vibration and noise through the proper use of materials and configurations to produce the increased damping properties.

In recent research, to make this attenuation more predictable, the most popular method is the application of high-damping materials, like viscoelastic substances to facilitate system damping. For almost half a century, researchers have conducted studies on different strategies and mathematical representations of the viscoelastic damping mechanism. These damping models include the simplest complex constant modulus model [1,2], the normal rheological model [3], the modal strain energy model [4], the derivative form model (like the fractional derivative model) [5], and the integral form model [6–11]. The important practical applications to damping structures are also reviewed by Rao [12].

Currently, many research interests concentrate on developing more sophisticated mathematical models that can be used in the analysis and design of complex structures that incorporate viscoelastic damping. The time-domain integral form and its counterpart in the frequency domain, which considers influencing factors such as temperature and frequency, are constantly being revised and improved. It is known that the time-domain ordinary differential equation (ODE), combined with the damping models expressed as the integral form, is more convenient to solve. Such proposed damping models are roughly classified into the anelastic displacement [6]/augmenting thermodynamic fields [7] model, the minioscillator type [Biot [8], the Golla–Hughes–McTavish (GHM) [9]], and the others (Yiu [10], Adhikari [11], etc).

Among the different viscoelastic damping treatments, that include the free layer treatment proposed by Plass [13] in 1957 and the constrained layered treatment proposed by Kerwin [14] in 1959, the constrained layer damping structures are the most efficient when introducing damping to the system. In the academic world, the six-order partial differential equation (PDE) of constrained layered beam, in terms of axial displacement, was developed by DiTaranto [15], and the similar PDE, in terms of transverse displacement, was derived by Mead and Markus [1] in 1969. Most of the basic research is accomplished on the three-layer constrained sandwich beam due to its ability to demonstrate the effects of various factors that influence system damping properties. To further attenuate the noise and vibration for the sandwich beam, increasing the number of layers is an excellent option. In the 1980s, the Hamilton's principle was used by Ma [16] to establish the closed-form solution for calculating the vibration damping problem of a five-layer simply-supported sandwich beam. Another work by Hao and Rao [2,17] applied the Hamilton's principle to extend the prediction scheme to the arbitrary number of layers in the system.

However, the inconvenience of having to rederive the system-governing equations for each change in the boundary condition is the major disadvantage of the closed-form solution. In recent years, the finite element (FE) method is becoming the most popular numerical scheme. This method is attractive for studying any arbitrary geometry

Received 12 March 2009; revision received 30 June 2009; accepted for publication 15 July 2009.

*Ph.D. Candidate, Mechanical Engineering Department; kevinlin@mtu.edu.

†Professor, Mechanical Engineering Department; mrao@mtu.edu.

and boundary by extending the academic work to the industrial problems. Further, the transient response of the damping structure is increasingly concerned with the arbitrary type of excitation. In 2006, Zhang et al. [18] studied the vibration performance of the FE-based three-layer sandwich structure by incorporating improved damping models of the viscoelastic materials. It is important to extend this work from the three-layer to the multiple-layered structure with the Biot damping model, as well as the combination of different damping material for the purpose of achieving optimum system damping and more adjustable temperature range of the high-damping performance. The objective of this paper is to present a complete numerical procedure on vibration design for a multiple-layer constrained damping beam by incorporating the Biot damping model. Results obtained from the numerical method are compared with the previous closed-form results to show the validity of this approach.

II. Finite Element Modeling of Multiple-Layer Beam

The modeling of the multiple-layer sandwich beam will be discussed in this section. The elastic beam and the constrained damping layer are two fundamental components in this modeling task. The concept of a transfer matrix is used to convert the local coordinates to the global coordinates. The two components are then assembled and used to construct the complete model of the structure with any number of layers. The approach is demonstrated for modeling beam structures. The technique can be applied to structures with a multiple-layered plate or shells in the same manner, as long as the system mass and stiffness matrices are made available. The following demonstrates the details for modeling the beam system.

A. Two Fundamental Components in a Multiple-Layer Beam

1. Modeling of the Elastic Layer

The FE model (FEM) shown in Fig. 1 contains two nodes and 6 degrees of freedom (DOF). The displacements of each node can be expressed as

$$\{\delta\}^e_{\text{elastic}} = \underbrace{(\,w_i \quad \theta_i \quad u_i \quad w_j \quad \theta_j \quad u_j\,)^T}_{6\times 1} \tag{1}$$

Therefore, the displacement of any point inside the element would be

$$\{u\}^e_{\text{elastic}} = \underbrace{(\,w \quad \theta \quad u\,)^T}_{3\times 1} = \underbrace{\begin{bmatrix} N_f \\ N'_f \\ N_e \end{bmatrix}}_{3\times 6} \underbrace{\{\delta\}^e_{\text{elastic}}}_{6\times 1} \tag{2}$$

where the shape functions are as follows:

$$[N_f] = [\,1-3\xi^2+2\xi^3 \quad (\xi-2\xi^2+\xi^3)l \quad 0 \quad 3\xi^2-2\xi^3 \quad (-\xi^2+\xi^3)l \quad 0\,]$$

$$[N'_f] = \left[\frac{\partial N_f}{\partial x}\right] = \frac{1}{l}\left[\frac{\partial N_f}{\partial \xi}\right] \qquad [N_e] = [\,0 \quad 0 \quad 1-\xi \quad 0 \quad 0 \quad \xi\,] \tag{3}$$

where $\xi = x/l$, $\xi \in [0,\ 1]$, and ξ stand for the local coordinate; the letter l is the length of the beam along x as the horizontal axis.

Next, the stiffness matrix can be derived based on the energy method:

$$[K_e]^e_{\text{elastic}} = \int_l [EA\varepsilon^2 + EI\varepsilon_\theta^2]\,\mathrm{d}x \tag{4}$$

where the first and second term in the integration are the extensional strain energy and the bending strain energy of the elastic layer, respectively.

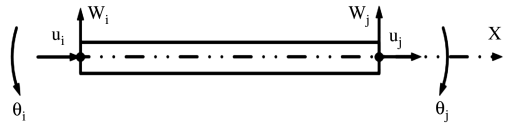

Fig. 1 Configuration of the elastic layer showing the DOF.

Applying the shape function [Eq. (3)] yields the element stiffness matrix in the local coordinate form:

$$[K_e]^e_{\text{elastic}} = \int_0^1 \frac{EA}{l} \underbrace{\left[\frac{\partial N_e}{\partial \xi}\right]^T}_{6\times 1} \underbrace{\left[\frac{\partial N_e}{\partial \xi}\right]}_{1\times 6} \mathrm{d}\xi + \underbrace{\int_0^1 \frac{EI}{l}\left[\frac{\partial^2 N_f}{\partial \xi^2}\right]^T \left[\frac{\partial^2 N_f}{\partial \xi^2}\right] \mathrm{d}\xi}_{6\times 6} \tag{5}$$

where A is the cross-sectional area of the elastic layer, E is Young's modulus of the elastic layer, l is the longitudinal length of the elastic layer, and I is the moment of inertia of the elastic layer.

Similarly, the element mass matrix can be expressed as

$$\underbrace{[M]^e_{\text{elastic}}}_{6\times 6} = \int_0^1 ml\Big(\underbrace{[N_f]^T}_{6\times 1} \underbrace{[N_f]}_{1\times 6} + [N_e]^T[N_e]\Big)\,\mathrm{d}\xi \tag{6}$$

where m is the mass of the unit length in this elastic layer.

2. Modeling of the Constrained Damping Layer

The construction of the FEM of the constrained damping beam containing the damping layer sandwiched between two outer layers is shown in Fig. 2. The major assumption of this three-layer structure is that these three layers share the identical transverse and rotational displacements; however, all three layers have different axial displacement, allowing the shear behavior of the constrained damping layer. Figure 2 illustrates this FEM, consisting of two nodes and 8 DOF in each element. The nodal displacement vector is

$$\{\delta\}^e_{\text{cons}} = \underbrace{(\,w_i \quad \theta_i \quad u_{1i} \quad u_{3i} \quad w_j \quad \theta_j \quad u_{1j} \quad u_{3j}\,)^T}_{8\times 1} \tag{7}$$

In Fig. 2, the top and bottom layers can be treated as the elastic layers, as discussed previously in this section. Because of the subordinate relationship of the nodal displacement between the three-layered 8 DOF sandwich element and the elastic layer element with 6 DOF, the element stiffness and mass matrix can be derived through a transportation matrix.

By comparing the nodal displacement of the elastic layer [Eq. (1)] and the constrained layer system [Eq. (7)], the mathematical relationship between the two vectors can be established as

$$\underbrace{\{\delta\}^e_{\text{elastic}}}_{6\times 1} = \underbrace{[T_1]}_{6\times 8} \underbrace{\{\delta\}^e_{\text{cons}}}_{8\times 1} \tag{8}$$

where the transfer matrix can be written as $[T_1] = [\,e_1 \quad e_2 \quad e_3 \quad e_5 \quad e_6 \quad e_7\,]^T$, and each e_i represents the following vector:

$$e_i = \Big(0 \quad 0 \quad \cdots \quad \cdots \quad \underbrace{1}_{i^{\text{th}}\text{place}} \quad \cdots \quad \cdots \quad 0\Big)^T \tag{9}$$

The dimension of the transfer matrix is purely determined by the DOF of the source, as well as the target nodal vector. Therefore, the element stiffness and the mass matrix of the top layer are readily calculated by $[T_1]^T[K_e]^e_{\text{elastic}}[T_1]$ and $[T_1]^T[M]^e_{\text{elastic}}[T_1]$.

The same procedure can be applied to the bottom layer, by means of the transfer matrix, as

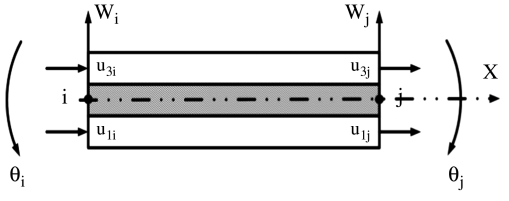

Fig. 2 Configuration of the constrained damping layer showing the DOF.

$$[T_3] = (\, e_1 \quad e_2 \quad e_4 \quad e_5 \quad e_6 \quad e_8 \,)^T$$
$$e_i = \Big(0 \quad 0 \quad \cdots \quad \cdots \quad \underbrace{1}_{i^{\text{th}}\text{place}} \quad \cdots \quad \cdots \quad 0\Big)^T \tag{10}$$

Neglecting the axial and bending strain energy of the viscoelastic damping layer in this three-layer structure, only the shear strain energy is taken into consideration when the element stiffness matrix of the damping layer is derived. Figure 3 visualizes the displacement relationship in this three-layer structure.

Here, u_A and u_B symbolize the horizontal displacement for the corner point of both elastic layers adjacent to the damping layer. In this three-layer element, u_1, u_2, and u_3 stand for the horizontal displacement for the base layer, the damping layer, and the constrained layer, and h_1, h_2, and h_3 are the thickness of the three different layers, respectively.

$$u_B = u_3 + \frac{\partial w}{\partial x}\frac{h_3}{2}; \qquad u_A = u_1 + \frac{\partial w}{\partial x}\frac{h_1}{2} \tag{11}$$

The rotational angle along the y axis for the damping layer, due to the axial mismatch of two elastic layers, is

$$\boldsymbol{\varphi} = \frac{u_B - u_A}{h_2} \tag{12}$$

Therefore, the total shear strain would be the accumulation of the $\boldsymbol{\varphi}$ and the angle which the consistent rotational angle contributes to the damping layer. Thus, the shear strain of the damping layer can be expressed as

$$\gamma_2 = \frac{u_3 - u_1}{h_2} + \frac{h_0}{h_2}\frac{\partial \omega}{\partial x}; \qquad h_0 = \frac{1}{2}(h_1 + h_3) + h_2 \tag{13}$$

By applying Eqs. (11–13), Eq. (13) yields the shape function:

$$\gamma_2 = \underbrace{\left[\frac{N_{e3} - N_{e1}}{h_2} + \frac{h_0}{h_2}\cdot\frac{1}{l}\cdot\frac{\partial N_{f1}}{\partial \xi}\right]^T}_{1\times 8} \cdot \underbrace{\{\delta\}^e_{\text{cons}}}_{8\times 1} \tag{14}$$

where

$$\underbrace{[N_{e1}]}_{1\times 8} = \underbrace{[N_e]}_{1\times 6}\underbrace{[T_1]}_{6\times 8}; \qquad [N_{e3}] = [N_e][T_3]$$
$$\lfloor N_{f1} \rfloor = \lfloor N_f \rfloor [T_1]$$

Accordingly, based on the energy method, the element viscoelastic stiffness matrix can be derived as

$$[K_v]^e_{\text{cons}} = \int_l \frac{1}{k} G A \gamma^2 \, \mathrm{d}x \tag{15}$$

where A_2 is the cross-sectional area of the damping layer, G_2 is the long-term shear modulus of the damping layer, and k is the correction factor of the shear strain energy for the rectangular cross section $k = 1.2$.

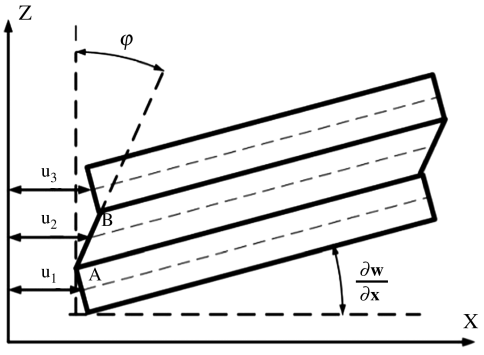

Fig. 3 Deformation relationship of the viscoelastic core.

Commonly, only the longitudinal kinetic energy needs to be considered, and the element mass matrix in this layer is

$$[M]^e_{\text{cons},2} = \int_0^1 m_2 l [N_{f1}]^T [N_{f1}] \, \mathrm{d}\xi \tag{16}$$

In summary, the element elastic stiffness, the element viscoelastic stiffness, and the element mass matrix for this three-layer component, respectively, are

$$[K_e]^e_{\text{cons}} = [T_1]^T \cdot [K_e]_{\text{elastic}} \cdot [T_1] + [T_3]^T \cdot [K_e]_{\text{elastic}} \cdot [T_3]$$
$$[K_v]^e_{\text{cons}} = \int_0^1 \frac{G_2 A_2 l}{k h_2}\left[\frac{N_{e3} - N_{e1}}{h_2} + \frac{h_0}{h_2}\cdot\frac{1}{l}\cdot\frac{\partial N_{f1}}{\partial \xi}\right]^T \times \left[\frac{N_{e3} - N_{e1}}{h_2} + \frac{h_0}{h_2}\cdot\frac{1}{l}\cdot\frac{\partial N_{f1}}{\partial \xi}\right] \mathrm{d}\xi \tag{17}$$

and

$$[M]^e_{\text{cons}} = [T_1]^T \cdot [M]_{\text{elastic}} \cdot [T_1] + [M]^e_{\text{cons},2} + [T_3]^T \cdot [M]_{\text{elastic}} \cdot [T_3]$$

B. Finite Element Modeling of a Seven-Layer Constrained Damping Beam

Any damping structure with an arbitrary number of layers can be constructed by the combination of the two fundamental components described previously. In terms of mathematical transformation through the transfer matrix, the stiffness and mass matrices of the multiple layer damping beam can be calculated by the element stiffness and the mass matrix of the elastic layer, as well as the constrained damping layers, as discussed in the previous section. This section demonstrates the procedure for building a seven-layer sandwich beam.

The seven-layer sandwich beam is composed of seven alternating layers, including four elastic layers and three damping layers. Figure 4 shows the construction of the FEM of a seven-layer sandwich beam, consistent with the assumption in the previous derivation. This FEM contains two nodes and 10 DOF, and the node displacement vector is

$$\{\boldsymbol{\delta}\}^e_{7\text{layer}} = \underbrace{(\, w_i \quad \theta_i \quad u_{1i} \quad u_{3i} \quad u_{5i} \quad u_{7i} \quad w_j \quad \theta_j \quad u_{1j} \quad u_{3j} \quad u_{5j} \quad u_{7j} \,)^T}_{12\times 1} \tag{18}$$

According to the previous discussion of Eq. (8), the transfer matrix is as follows to obtain the element stiffness and the mass matrix when the first, third, fifth, and seventh layer are elastic layers:

$$[\mathbf{T_1}] = \underbrace{(\, \mathbf{e_1} \quad \mathbf{e_2} \quad \mathbf{e_3} \quad \mathbf{e_7} \quad \mathbf{e_8} \quad \mathbf{e_9} \,)^{\mathbf{T}}}_{\mathbf{6\times 12}}$$
$$[\mathbf{T_3}] = \underbrace{(\, \mathbf{e_1} \quad \mathbf{e_2} \quad \mathbf{e_4} \quad \mathbf{e_7} \quad \mathbf{e_8} \quad \mathbf{e_{10}} \,)^{\mathbf{T}}}_{\mathbf{6\times 12}}$$
$$[\mathbf{T_5}] = \underbrace{(\, \mathbf{e_1} \quad \mathbf{e_2} \quad \mathbf{e_5} \quad \mathbf{e_7} \quad \mathbf{e_8} \quad \mathbf{e_{11}} \,)^{\mathbf{T}}}_{\mathbf{6\times 12}}$$
$$[\mathbf{T_7}] = \underbrace{(\, \mathbf{e_1} \quad \mathbf{e_2} \quad \mathbf{e_6} \quad \mathbf{e_7} \quad \mathbf{e_8} \quad \mathbf{e_{12}} \,)^{\mathbf{T}}}_{\mathbf{6\times 12}} \tag{19}$$

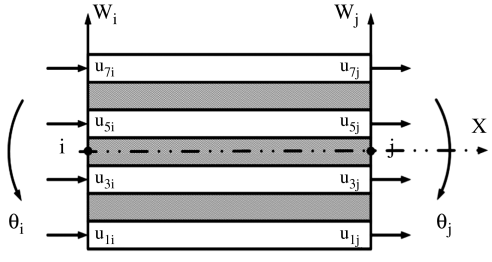

Fig. 4 Configuration of a seven-layer damping structure showing the DOF.

Similarly, the element stiffness and the mass matrix for the second, fourth, and sixth layers, as the constrained damping layer, can be derived through the transfer matrix as follows:

$$[\mathbf{T_2}] = \underbrace{(\mathbf{e_1} \quad \mathbf{e_2} \quad \mathbf{e_3} \quad \mathbf{e_4} \quad \mathbf{e_7} \quad \mathbf{e_8} \quad \mathbf{e_9} \quad \mathbf{e_{10}})^{\mathbf{T}}}_{\mathbf{8\times 12}}$$

$$[\mathbf{T_4}] = \underbrace{(\mathbf{e_1} \quad \mathbf{e_2} \quad \mathbf{e_4} \quad \mathbf{e_5} \quad \mathbf{e_7} \quad \mathbf{e_8} \quad \mathbf{e_{10}} \quad \mathbf{e_{11}})^{\mathbf{T}}}_{\mathbf{8\times 12}}$$

$$[\mathbf{T_6}] = \underbrace{(\mathbf{e_1} \quad \mathbf{e_2} \quad \mathbf{e_5} \quad \mathbf{e_6} \quad \mathbf{e_7} \quad \mathbf{e_8} \quad \mathbf{e_{11}} \quad \mathbf{e_{12}})^{\mathbf{T}}}_{\mathbf{8\times 12}} \tag{20}$$

where the notation e_i represents

$$\mathbf{e_i} = \underbrace{\left(0 \quad 0 \quad \cdots \quad \cdots \quad \underbrace{1}_{i^{\text{th}}\text{place}} \quad \cdots \quad \cdots \quad 0\right)^T}_{12\times 1} \tag{21}$$

In summary, based on the former equations (and with the parameters of each layer), the element mass/stiffness/damping matrix of the seven-layer sandwich damping beam can be expressed as

$$[\mathbf{K_e}]^e = \mathbf{T_1^T}[\mathbf{K_{e1}}]\mathbf{T_1} + \mathbf{T_3^T}[\mathbf{K_{e3}}]\mathbf{T_3} + \mathbf{T_5^T}[\mathbf{K_{e5}}]\mathbf{T_5} + \mathbf{T_7^T}[\mathbf{K_{e7}}]\mathbf{T_7}$$

$$[\mathbf{K}_v]^e = \mathbf{T_2^T}[\mathbf{K}_{v2}]\mathbf{T}_2 + \mathbf{T_4^T}[\mathbf{K}_{v4}]\mathbf{T}_4 + \mathbf{T_6^T}[\mathbf{K}_{v6}]\mathbf{T}_6$$

$$[\mathbf{M_e}]^e = \sum_{i=1}^{7} \mathbf{T_i^T}[\mathbf{M_{ei}}]\mathbf{T_i} \tag{22}$$

Assembling the element matrices and applying the boundary condition by the conventional FE technique [19], the global mass/stiffness/damping matrix can be obtained. When taking the viscoelastic damping properties into consideration, the global matrices need to be constructed. The dynamic equation and its solution will be discussed in the next section.

III. Derivation of the Biot Dynamic Equation

The purpose of this section is to incorporate the damping properties into the discretized system using the technique discussed in the previous section. Unlike the frequency domain damping model in previous studies, this section demonstrates the time-domain Biot damping model with its ability to employ different viscoelastic materials in a damping structure.

The dynamic equation discretized by a numerical implementation, such as the FEM, can be expressed in the following second-order ODE form, with M, C, and K representing the global mass, damping, and stiffness matrices, respectively:

$$\mathbf{M}\,\ddot{\mathbf{x}} + \mathbf{C}\dot{\mathbf{x}} + \mathbf{K}\mathbf{x} = \mathbf{f(t)} \tag{23}$$

By applying the constitutive relationship for the two different damping materials, with the hereditary integral form, to the previous equation, the discretized dynamic equation becomes

$$\mathbf{M}\ddot{\mathbf{x}} + \mathbf{K_e}\mathbf{x} + \mathbf{K_{v1}}\left[G_1(t)\mathbf{x}(0) + \int_0^t G_1(t-\tau)\dot{\mathbf{x}}\,\mathrm{d}\tau\right] + \mathbf{K_{v2}}\left[G_2(t)\mathbf{x}(0) + \int_0^t G_2(t-\tau)\dot{\mathbf{x}}\,\mathrm{d}\tau\right] = \mathbf{f}(t) \tag{24}$$

In other words, this dynamic system contains two types of viscoelastic damping material, where K_e stands for the elastic stiffness matrix due to the axial and bending strain energy and K_{v1} and K_{v2} symbolize the damping matrix of two different types of damping materials.

Then, the dynamic equation will take the following form by using the Laplace transform:

$$[s^2\mathbf{M} + \mathbf{K_e} + s\tilde{G}_1(s)\mathbf{K_{v1}} + s\tilde{G}_2(s)\mathbf{K_{v2}}]\mathbf{X}(s) = \mathbf{F}(s) \tag{25}$$

Where s stands for the Laplace variable ($s = \sigma + j\omega$), and the $sG_i(s)$ is the core function of the complex shear modulus for the ith type of viscoelastic material. In this paper, the Biot viscoelastic damping model will be used, and its complex shear modulus, with the series of minioscillator perturbing term [8], can be expressed as

$$s\tilde{G}(s) = G^{\infty}\left[1 + \sum_{k=1}^{m} a_k \frac{s}{s+b_k}\right] \tag{26}$$

where G^{∞} is the long-term shear moduli, and a_k and b_k are the Biot constants. These parameters are positive and can be determined by the nonlinear curve fitting from experimental data. Because of the simplification purpose, the number of perturbing terms is assumed to be one, and the complex modulus functions of two different viscoelastic materials are

$$s\tilde{G}_1(s) = G_1^{\infty}\left[1 + a_1\frac{s}{s+b_1}\right]$$

$$s\tilde{G}_2(s) = G_2^{\infty}\left[1 + a_2\frac{s}{s+b_2}\right] \tag{27}$$

Applying Eqs. (25–27) and rearranging the terms yield:

$$\left\{s^2\mathbf{M} + \mathbf{Ke} + \left[G_1^{\infty}(1+a_1) - G_1^{\infty}\frac{a_1b_1}{s+b_1}\right]\mathbf{K_{v1}} + \left[G_2^{\infty}(1+a_2) - G_2^{\infty}\frac{a_2b_2}{s+b_2}\right]\mathbf{K_{v2}}\right\}\mathbf{X}(s) = \mathbf{F}(s) \tag{28}$$

The following procedure will introduce the dissipation coordinates into the dynamic equation in order to eliminate the Laplace variable s in the previous equation, to gain the frequency independence by increasing the number of unknowns in the dynamic equation. In this case, the number of dissipation coordinates needs to be equal to one, because the number of perturbing terms is assumed to be one. Therefore, the dissipation coordinates for the two types of damping material are

$$\hat{\mathbf{Z}}_1(s) = \frac{b_1}{s+b_1}\mathbf{X}(s) \Rightarrow \dot{\hat{\mathbf{z}}}_1 + b_1\hat{\mathbf{Z}}_1 = b_1\mathbf{x}$$

$$\hat{\mathbf{Z}}_2(s) = \frac{b_2}{s+b_2}\mathbf{X}(s) \Rightarrow \dot{\hat{\mathbf{z}}}_2 + b_2\hat{\mathbf{Z}}_2 = b_2\mathbf{x} \tag{29}$$

Combine Eqs. (28) and (29) to form a simultaneous equation system and take the inverse Laplace transform:

$$\begin{cases} \mathbf{M}\ddot{\mathbf{x}} + [\mathbf{K_e} + G_1^{\infty}(1+a_1)\mathbf{K_{v1}} + G_2^{\infty}(1+a_2)\mathbf{K_{v2}}]\mathbf{x} - G_1^{\infty}a_1\mathbf{K_{v1}}\hat{\mathbf{Z}}_1 - G_2^{\infty}a_2\mathbf{K_{v2}}\hat{\mathbf{Z}}_2 = \mathbf{f}(t) \\ -b_1\mathbf{x} + \dot{\hat{\mathbf{z}}}_1 + b_1\hat{\mathbf{Z}}_1 = 0 \\ -b_2\mathbf{x} + \dot{\hat{\mathbf{z}}}_2 + b_2\hat{\mathbf{Z}}_2 = 0 \end{cases} \tag{30}$$

Table 1 Biot constants of 3M ISD-110 at 45°C

Parameter	Value	Parameter	Value
G^{∞}	55,000 Pa	b_1	5.410993
a_1	1.809517	b_2	1093.778
a_2	14.53095	b_3	60.36544
a_3	3.221535	b_4	4319.613
a_4	52.01026	b_5	2840958
a_5	19768.22	b_6	298.0672
a_6	6.561162		

The auxiliary equation obtained from the introduction of the dissipation coordinate will be transformed to form the symmetric stiffness matrix of Eq. (31):

$$\frac{1}{b_1}\dot{\hat{\mathbf{z}}}_1 + \hat{\mathbf{Z}}_1 - \mathbf{x} = 0 \Rightarrow \underbrace{\frac{1}{b_1}[\mathbf{R}_{v1}^{\mathrm{T}}]^{-1}\dot{\mathbf{z}}_1 + [\mathbf{R}_{v1}^{\mathrm{T}}]^{-1}\mathbf{z}_1 - \mathbf{x} = 0}_{\times G_1^{\infty} a_1 \mathbf{\Lambda}_{v1}\mathbf{R}_{v1}^{\mathrm{T}}}$$

$$\Rightarrow G_1^{\infty}\frac{a_1}{b_1}\mathbf{\Lambda}_{v1}\dot{\mathbf{z}}_1 + G_1^{\infty}a_1\mathbf{\Lambda}_{v1}\mathbf{z}_1 - G_1^{\infty}a_1\mathbf{\Lambda}_{v1}\mathbf{R}_{v1}^{\mathrm{T}}\mathbf{x} = 0$$

Rewrite the equation system as the matrix form:

$$\begin{bmatrix} \mathbf{M} & & \\ & \mathbf{0} & \\ & & \mathbf{0} \end{bmatrix}\begin{Bmatrix} \ddot{\mathbf{x}} \\ \ddot{\hat{\mathbf{z}}}_1 \\ \ddot{\hat{\mathbf{z}}}_2 \end{Bmatrix} + \begin{bmatrix} 0 & & \\ & \mathbf{I} & \\ & & \mathbf{I} \end{bmatrix}\begin{Bmatrix} \dot{\mathbf{x}} \\ \dot{\hat{\mathbf{z}}}_1 \\ \dot{\hat{\mathbf{z}}}_2 \end{Bmatrix} + \begin{bmatrix} \mathbf{K_e} + G_1^{\infty}(1+a_1)\mathbf{K_{v1}} + G_2^{\infty}(1+a_2)\mathbf{K_{v2}} & -G_1^{\infty}a_1\mathbf{K_{v1}} & -G_2^{\infty}a_2\mathbf{K_{v2}} \\ -b_1\mathbf{I} & b_1\mathbf{I} & \mathbf{0} \\ -b_2\mathbf{I} & \mathbf{0} & b_2\mathbf{I} \end{bmatrix}\begin{Bmatrix} \mathbf{x} \\ \hat{\mathbf{Z}}_1 \\ \hat{\mathbf{Z}}_2 \end{Bmatrix} = \begin{Bmatrix} \mathbf{f} \\ 0 \\ 0 \end{Bmatrix} \quad (31)$$

The stiffness matrix in the Eq. (31) needs to be symmetric for further analysis according to the Maxwell principle. The mathematical manipulation will be performed to obtain the equivalent symmetric matrix. The nomenclature applied to two different damping materials, respectively, is defined as:

$$\mathbf{K_{v1}} = \mathbf{R_{v1}}\mathbf{\Lambda_{v1}}\mathbf{R_{v1}^{\mathrm{T}}}; \qquad \mathbf{K_{v2}} = \mathbf{R_{v2}}\mathbf{\Lambda_{v2}}\mathbf{R_{v2}^{\mathrm{T}}}; \qquad \mathbf{z_1} = \mathbf{R_{v1}^{\mathrm{T}}}\hat{\mathbf{Z}}_1$$
$$\mathbf{z_2} = \mathbf{R_{v2}^{\mathrm{T}}}\hat{\mathbf{Z}}_2 \Rightarrow \hat{\mathbf{Z}}_1 = [\mathbf{R_{v1}^{\mathrm{T}}}]^{-1}\mathbf{z_1}; \qquad \hat{\mathbf{Z}}_2 = [\mathbf{R_{v2}^{\mathrm{T}}}]^{-1} \quad (32)$$

where Λ_{vi} and R_{vi} are the diagonal eigenvalue and the eigenvector matrix of the damping stiffness matrix as K_{vi}.

Similarly,

$$\frac{1}{b_2}\dot{\hat{\mathbf{z}}}_2 + \hat{\mathbf{z}}_2 - \mathbf{x} = 0 \Rightarrow G_2^{\infty}\frac{a_2}{b_2}\mathbf{\Lambda_{v2}}\dot{\mathbf{z}}_2 - G_2^{\infty}a_2\mathbf{\Lambda_{v2}}\mathbf{R_{v2}^{\mathrm{T}}}\mathbf{x} = 0 \quad (33)$$

Now, with Eq. (33), the simultaneous equation system can be rewritten with the symmetric stiffness matrix as

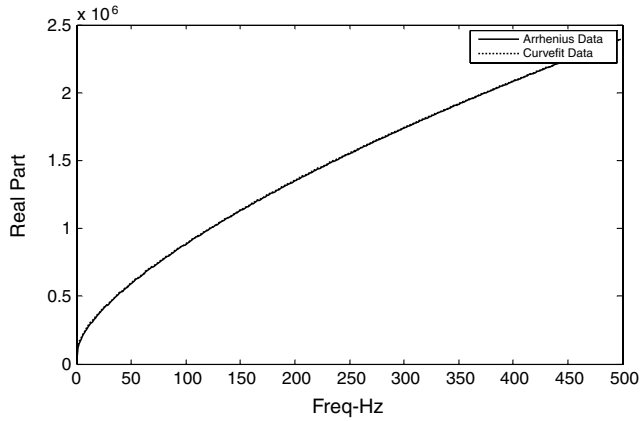

a)

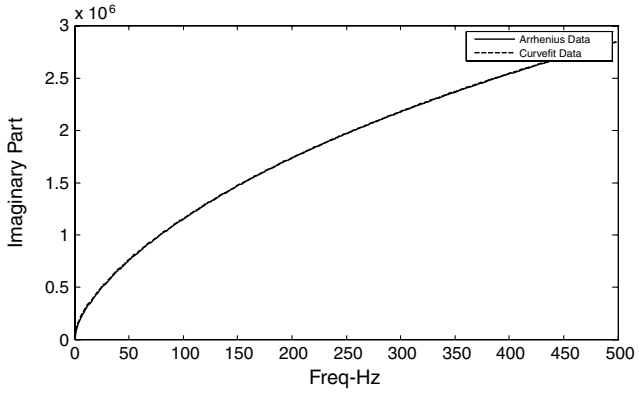

b)

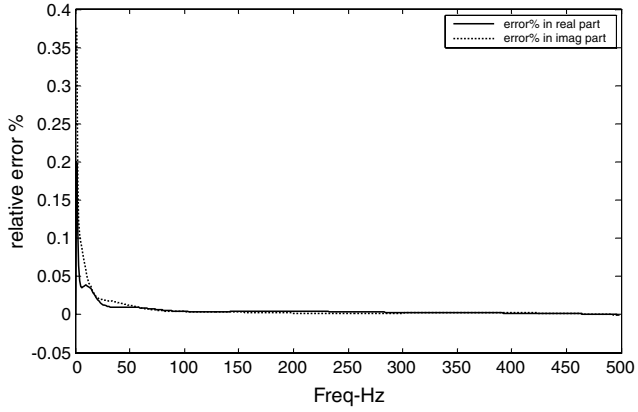

c)

Fig. 5 Comparison of a) real part of shear modulus, b) imaginary part of shear modulus, and c) relative error percentage for 3M ISD-100 material at 45°C.

$$\underbrace{\begin{bmatrix}\mathbf{M} & & \\ & \mathbf{0} & \\ & & \mathbf{0}\end{bmatrix}}_{M}\begin{Bmatrix}\ddot{\mathbf{x}}\\ \ddot{\mathbf{z}}_1\\ \ddot{\mathbf{z}}_2\end{Bmatrix}+\underbrace{\begin{bmatrix}0 & 0 & 0\\ 0 & G_1^{\infty}\frac{a_1}{b_1}\mathbf{\Lambda}_{\mathbf{v1}} & 0\\ 0 & 0 & G_2^{\infty}\frac{a_2}{b_2}\mathbf{\Lambda}_{\mathbf{v2}}\end{bmatrix}}_{D}\begin{Bmatrix}\mathbf{x}\\ \dot{\mathbf{z}}_1\\ \dot{\mathbf{z}}_2\end{Bmatrix}$$
$$+\underbrace{\begin{bmatrix}\mathbf{K_e}+G_1^{\infty}(1+a_1)\mathbf{K_{v1}}+G_2^{\infty}(1+a_2)\mathbf{K_{v2}} & -G_1^{\infty}a_1\mathbf{R_{v1}}\mathbf{\Lambda_{v1}} & -G_2^{\infty}a_2\mathbf{R_{v2}}\mathbf{\Lambda_{v2}}\\ -G_1^{\infty}a_1\mathbf{\Lambda_{v1}}\mathbf{R}_{\mathbf{v1}}^{T} & G_1^{\infty}a_1\mathbf{\Lambda_{v1}} & \mathbf{0}\\ -G_2^{\infty}a_2\mathbf{\Lambda_{v2}}\mathbf{R}_{\mathbf{v2}}^{T} & \mathbf{0} & G_2^{\infty}a_2\mathbf{\Lambda_{v2}}\end{bmatrix}}_{K}\begin{Bmatrix}\mathbf{x}'\\ \mathbf{z}'_1\\ \mathbf{z}'_2\end{Bmatrix}=\begin{Bmatrix}\mathbf{f}\\ 0\\ 0\end{Bmatrix} \tag{34}$$

The following additional nomenclature needs to be used in order to simplify Eq. (34):

$$G_1^{\infty}\mathbf{\Lambda_{v1}}=\mathbf{\Lambda_1};\qquad G_2^{\infty}\mathbf{\Lambda_{v2}}=\mathbf{\Lambda_2}$$
$$G_1^{\infty}\mathbf{R_{v1}}\mathbf{\Lambda_{v1}}=\mathbf{R_1}\Rightarrow\mathbf{R}_1^{T}=G_1^{\infty}\mathbf{\Lambda}_{\mathbf{v1}}^{\mathbf{T}}\mathbf{R}_{\mathbf{v1}}^{\mathbf{T}}$$
$$G_2^{\infty}\mathbf{R_{v2}}\mathbf{\Lambda_{v2}}=\mathbf{R_2}\Rightarrow\mathbf{R}_2^{\mathbf{T}}=G_2^{\infty}\mathbf{\Lambda}_{\mathbf{v2}}^{\mathbf{T}}\mathbf{R}_{\mathbf{v2}}^{\mathbf{T}} \tag{35}$$

Thus, the dynamic equation applied to the Biot damping model (assuming one perturbing term) with two different damping materials can be manipulated as the symmetric form:

$$\underbrace{\begin{bmatrix}\mathbf{M} & & \\ & \mathbf{0} & \\ & & \mathbf{0}\end{bmatrix}}_{\tilde{\mathbf{M}}}\begin{Bmatrix}\ddot{\mathbf{x}}\\ \ddot{\mathbf{z}}_1\\ \ddot{\mathbf{z}}_2\end{Bmatrix}+\underbrace{\begin{bmatrix}0 & 0 & 0\\ 0 & \frac{a_1}{b_1}\mathbf{\Lambda}_1 & 0\\ 0 & 0 & \frac{a_2}{b_2}\mathbf{\Lambda}_2\end{bmatrix}}_{\tilde{\mathbf{D}}}\begin{Bmatrix}\mathbf{x}\\ \dot{\mathbf{z}}_1\\ \dot{\mathbf{z}}_2\end{Bmatrix}+\underbrace{\begin{bmatrix}\mathbf{K_e}+G_1^{\infty}(1+a_1)\mathbf{K_{v1}}+G_2^{\infty}(1+a_2)\mathbf{K_{v2}} & -a_1\mathbf{R_1} & -a_2\mathbf{R_2}\\ -a_1\mathbf{R}_1^{\mathbf{T}} & a_1\mathbf{\Lambda_1} & \mathbf{0}\\ -a_2\mathbf{R}_2^{\mathbf{T}} & \mathbf{0} & a_2\mathbf{\Lambda_2}\end{bmatrix}}_{\tilde{\mathbf{K}}}\begin{Bmatrix}\mathbf{x}'\\ \mathbf{z}'_1\\ \mathbf{z}'_2\end{Bmatrix}=\underbrace{\begin{Bmatrix}\mathbf{f}\\ 0\\ 0\end{Bmatrix}}_{\tilde{\mathbf{f}}} \tag{36}$$

if the number of perturbing terms is extended from one to infinite, defining $a_{11}, \ldots, a_{1m}$; $b_{11}, \ldots, b_{1m}$; and $z_{11}, \ldots, z_{1m}$ as m terms of the Biot parameters and the dissipative coordinates, respectively, for the first viscoelastic material.

Similarly, $a_{21}, \ldots, a_{2n}$; $b_{21}, \ldots, b_{2n}$; and $z_{21}, \ldots, z_{2n}$ as n terms of the Biot parameters and the dissipation coordinates, respectively, for the second viscoelastic material.

Therefore, the dynamic equation with m terms of the Biot parameters for the first viscoelastic material and n terms of the second will become as follows:

$$\underbrace{\begin{bmatrix}\mathbf{M} & \mathbf{0} & \ldots & \mathbf{0} & \mathbf{0} & \ldots & \mathbf{0}\\ \mathbf{0} & \mathbf{0} & \ldots & \mathbf{0} & \mathbf{0} & \ldots & \mathbf{0}\\ \vdots & \vdots & \ddots & \vdots & \vdots & \ddots & \vdots\\ \mathbf{0} & \mathbf{0} & \ldots & \mathbf{0} & \mathbf{0} & \ldots & \mathbf{0}\\ \mathbf{0} & \mathbf{0} & \ldots & \mathbf{0} & \mathbf{0} & \ldots & \mathbf{0}\\ \vdots & \vdots & \ddots & \vdots & \vdots & \ddots & \vdots\\ \mathbf{0} & \mathbf{0} & \ldots & \mathbf{0} & \mathbf{0} & \ldots & \mathbf{0}\end{bmatrix}}_{\tilde{\mathbf{M}}}\underbrace{\begin{Bmatrix}\ddot{\mathbf{x}}\\ \ddot{\mathbf{z}}_{\mathbf{11}}\\ \vdots\\ \ddot{\mathbf{z}}_{\mathbf{1m}}\\ \ddot{\mathbf{z}}_{\mathbf{21}}\\ \vdots\\ \ddot{\mathbf{z}}_{\mathbf{2n}}\end{Bmatrix}}_{\ddot{\mathbf{q}}}+\underbrace{\begin{bmatrix}\mathbf{0} & \mathbf{0} & \ldots & \mathbf{0} & \mathbf{0} & \ldots & \mathbf{0}\\ \mathbf{0} & \frac{a_{11}}{b_{11}}\mathbf{\Lambda}_1 & \ldots & \mathbf{0} & \mathbf{0} & \ldots & \mathbf{0}\\ \vdots & \vdots & \ddots & \vdots & \vdots & \ddots & \vdots\\ \mathbf{0} & \mathbf{0} & \ldots & \frac{a_{1m}}{b_{1m}}\mathbf{\Lambda}_1 & \mathbf{0} & \ldots & \mathbf{0}\\ \mathbf{0} & \mathbf{0} & \ldots & \mathbf{0} & \frac{a_{21}}{b_{21}}\mathbf{\Lambda}_2 & \ldots & \mathbf{0}\\ \vdots & \vdots & \ddots & \vdots & \vdots & \ddots & \vdots\\ \mathbf{0} & \mathbf{0} & \ldots & \mathbf{0} & \mathbf{0} & \ldots & \frac{a_{2n}}{b_{2n}}\mathbf{\Lambda}_2\end{bmatrix}}_{\tilde{\mathbf{D}}}\underbrace{\begin{bmatrix}\dot{\mathbf{x}}\\ \dot{\mathbf{z}}_{\mathbf{11}}\\ \vdots\\ \dot{\mathbf{z}}_{\mathbf{1m}}\\ \dot{\mathbf{z}}_{\mathbf{21}}\\ \vdots\\ \dot{\mathbf{z}}_{\mathbf{2n}}\end{bmatrix}}_{\dot{\mathbf{q}}}$$
$$+\underbrace{\begin{bmatrix}\mathbf{K_e}+G_1^{\infty}(1+\sum_{k=1}^{m}a_{1k})\mathbf{K_{v1}}+G_2^{\infty}(1+\sum_{j=1}^{n}a_{2j})\mathbf{K_{v2}} & -a_{11}\mathbf{R_1} & \ldots & -a_{1m}\mathbf{R_1} & -a_{21}\mathbf{R_2} & \ldots & -a_{2n}\mathbf{R_2}\\ -a_{11}\mathbf{R}_1^{\mathbf{T}} & a_{11}\mathbf{\Lambda_1} & \ldots & \mathbf{0} & \mathbf{0} & \ldots & \mathbf{0}\\ \vdots & \vdots & \ddots & \vdots & \vdots & \ddots & \vdots\\ -a_{1m}\mathbf{R}_1^{\mathbf{T}} & \mathbf{0} & \ldots & a_{1m}\mathbf{\Lambda_1} & \mathbf{0} & \ldots & \mathbf{0}\\ -a_{21}\mathbf{R}_2^{\mathbf{T}} & \mathbf{0} & \ldots & \mathbf{0} & a_{21}\mathbf{\Lambda_2} & \ldots & \mathbf{0}\\ \vdots & \vdots & \ddots & \vdots & \vdots & \ddots & \vdots\\ -a_{2n}\mathbf{R}_2^{\mathbf{T}} & \mathbf{0} & \ldots & \mathbf{0} & \mathbf{0} & \ldots & a_{2n}\mathbf{\Lambda_2}\end{bmatrix}}_{\tilde{\mathbf{K}}}\underbrace{\begin{bmatrix}\mathbf{x}\\ \mathbf{z}_{\mathbf{11}}\\ \vdots\\ \mathbf{z}_{\mathbf{1m}}\\ \mathbf{z}_{\mathbf{21}}\\ \vdots\\ \mathbf{z}_{\mathbf{2n}}\end{bmatrix}}_{\mathbf{q}}=\underbrace{\begin{Bmatrix}\mathbf{f}\\ \mathbf{0}\\ \vdots\\ \mathbf{0}\\ \mathbf{0}\\ \vdots\\ \mathbf{0}\end{Bmatrix}}_{\tilde{\mathbf{f}}} \tag{37}$$

Supposing N is the number of DOF for the mass, stiffness, and damping matrix, the dimension of each square matrix in the previous equation is $(m + n + 1)N$ and the q vector stands for the unknowns, especially the x vector as the system displacement response.

In summary, by introducing the Biot damping model to apply the viscoelastic properties of a discretized system, a nonlinear ODE [Eq. (24)] transformed to a linear second-order ODE [Eq. (37)]. Solving the eigenvalue problem based on Eq. (37) determines the vibration characteristics of the system, such as natural frequency, loss factor, and complex mode shape.

Additionally, Eq. (37) may easily be extended from two types of viscoelastic materials to the infinite type in the same manner, using Eqs. (24–37). Thus, the dimension of the square matrix in the Biot dynamic equation with the infinite type of viscoelastic material is (1 + Σ number of Biot terms for all the materials) N.

IV. Parametric Determination of the Biot Damping Model

The proper use of the curve-fitting technique in providing the accurate Biot constants to the Biot dynamic equation is important.

Generally speaking, the dynamic characteristics of the viscoelastic materials can be obtained from an experimental method. It is known that the curve-fitting technique is normally employed to establish the connection between the experiment and the mathematical damping models. In this section, the nonlinear curve-fitting procedure of the complex shear modulus in the frequency domain is converted into a nonlinear constrained optimization problem.

Recalling Eq. (26) from Sec. II, the complex shear modulus with the Biot form in the frequency domain can be also written as real and imaginary parts separately:

$$s\tilde{G}(j\omega) = G^{\infty}\left[1 + \sum_{i=1}^{N} \frac{a_i \varpi^2}{b_i^2 + \varpi^2}\right] + jG^{\infty}\left[1 + \sum_{i=1}^{N} \frac{a_i b_i \varpi}{b_i^2 + \varpi^2}\right] \quad (38)$$

The Biot parameters, including G^{∞}, a_i and b_i, are estimated from the experimental data with the certain fit range of the frequency, both on the real part and the imaginary parts. The number of Biot perturbing items is given by N, an integral constant, defining the capability of this numerical approximation. In general, the different temperature is causing the change of the Biot parameters in the previous equation, and one set of Biot parameters needs to be determined in each ambient temperature independently.

Assuming $x_1 = G^{\infty}$, $x_2 = a_1$, $x_3 = b_1$, $x_4 = a_2$, and $x_5 = b_2$, $\cdots$ with the constraint condition $xk \geq 0$ and $k = 1, 2, \cdots$, num, the objective equation of this optimization problem can be expressed as:

$$\min_{x} F(x) = \sum_{j=1}^{P} |G_j^*(x) - G_{0j}|^2 \quad (39)$$

from the previous objective equation: G_{0j} stands for the complex shear modulus from the experimental data with the P interested points, and the value of P needs to be bigger than the number of unknowns in this optimization problem.

The following demonstrates the actual curve-fitting procedure. The 3M ISD-110 viscoelastic polymer is selected to verify the effectiveness of this procedure. The experimental data are given in the form of and Arrhenius empirical equation in the Appendix. Assuming T is equal to 45°C, and the fit range is 500 Hz, the complex shear modulus can be synthesized from the set of Arrhenius coefficients from Table A1 in the Appendix and from calculating the complex shear modulus through Eqs. (A1–A5). Once the experimental data are given, the number of terms in Eq. (38) needs to be determined to ensure the precision of this approximation. The commercial software package Auto2fit is used in this example, because it is capable of curve fitting the experimental data on both the real and imaginary parts simultaneously. Continuing to increase the Biot terms (N), the relative error between the Arrhenius and the curve-fitting results reduces, yet more computational effort is evidently also needed. With the compromised number of Biot terms equal to six, the eventual results are listed in Table 1.

Figures 5a and 5b show the real part and the imaginary part compared between the Arrhenius data and the curve-fitting data in this case.

As shown in the previous plots, the dynamic properties of the 3M ISD-110 at 45°C can be represented using the Biot parametric determination technique discussed in this section. The relative error between two sets of data is low, and the higher-frequency region contains almost zero error.

V. Decoupling Transformation and Dynamic Solution

The procedure of the complex eigenvalue and the time-domain transient response will be established with respect to the vibration problem for a multiple-layer viscoelastic damping structure in this section. In general, if the damping matrix C has the following proportional relationship with the mass matrix M and the stiffness matrix K,

$$\mathbf{C} = \alpha\mathbf{M} + \beta\mathbf{K} \quad (40)$$

and the modal damping matrix will be diagonal, where α and β are the proportional damping constants. Obviously, the damping matrix $\bar{\mathbf{D}}$ in Eq. (37) does not have the proportional relationship with the mass and stiffness matrix. Therefore, the decoupling transformation is needed for Eq. (37) to construct the first-order state equation by introducing the auxiliary equation $\mathbf{M}\dot{\mathbf{q}} - \mathbf{M}\dot{\mathbf{q}} = \mathbf{0}$ as:

$$\mathbf{A}\,\dot{\mathbf{y}} + \mathbf{B}\mathbf{y} = \hat{\mathbf{f}} \quad (41)$$

where

$$\mathbf{A} = \begin{bmatrix} \bar{\mathbf{D}} & \bar{\mathbf{M}} \\ \bar{\mathbf{M}} & \mathbf{0} \end{bmatrix}; \qquad \mathbf{B} = \begin{bmatrix} \bar{\mathbf{K}} & \mathbf{0} \\ \mathbf{0} & -\bar{\mathbf{M}} \end{bmatrix}; \qquad \mathbf{y} = \begin{Bmatrix} \mathbf{q} \\ \dot{\mathbf{q}} \end{Bmatrix}$$
$$\hat{\mathbf{f}} = \begin{Bmatrix} \bar{\mathbf{f}} \\ \mathbf{0} \end{Bmatrix} \quad (42)$$

If N is the number of DOF in the $\bar{\mathbf{M}}$, $\bar{\mathbf{D}}$, and $\bar{\mathbf{K}}$ matrices, the DOF of the A and $\boldsymbol{B}$ matrices will be $2N$.

First, the free vibration of Eq. (41) will be considered. Assuming $\hat{\mathbf{f}} = 0$, the following form of solution yields

$$(\mathbf{A}\boldsymbol{\lambda} + \mathbf{B}\mathbf{y})\boldsymbol{\Phi} = \mathbf{0} \quad (43a)$$

or

$$(\mathbf{A}\boldsymbol{\lambda} + \mathbf{B}\mathbf{y})\begin{Bmatrix} \boldsymbol{\Psi} \\ \boldsymbol{\Psi}\boldsymbol{\lambda} \end{Bmatrix} = \mathbf{0} \quad (43b)$$

Where the $\boldsymbol{\lambda}$ matrix stands for the $2N$ complex conjugate eigenvalues, including the natural frequencies and the loss factors information:

$$\begin{bmatrix} \ddots & & \\ & \boldsymbol{\lambda} & \\ & & \ddots \end{bmatrix} = \begin{bmatrix} \lambda_1 & & & \\ & \lambda_1^* & & 0 \\ & & \ddots & \\ & 0 & & \lambda_N \\ & & & & \lambda_N^* \end{bmatrix} \quad (44)$$

It noted that the zero items will appear in the eigenvalue matrix if the damping matrix $\bar{\mathbf{D}}$ is not fully ranked. The mode shape vector $\boldsymbol{\Psi}$ for the vector $\boldsymbol{q}$ can be extracted from the eigenvector matrix $\boldsymbol{\Phi}$ with respect to the vector $\boldsymbol{y}$:

$$[\Phi] = \begin{Bmatrix} [\Psi]_1 & [\Psi]_1^* & \cdots & [\Psi]_N & [\Psi]_N^* \\ \lambda_1[\Psi]_1 & \lambda_1^*[\Psi]_1^* & \cdots & \lambda_N[\Psi]_N & \lambda_N^*[\Psi]_N^* \end{Bmatrix} \quad (45)$$

In addition, Eq. (43) can be numerically solved by $\lambda\{\Psi\} = -[\mathbf{A}]^{-1}[\mathbf{B}]\{\Psi\}$ using a mathematical software package, such as MATLAB or Mathematica.

Second, the forced vibration solution of Eq. (41) in the time domain will be discussed. Supposing $\hat{\mathbf{f}} = \begin{Bmatrix} \mathbf{F} \\ \mathbf{0} \end{Bmatrix}$, the variable substitution can be made by assuming $\mathbf{y} = \boldsymbol{\Phi}\mathbf{p}$ and converting the state-space equation from the time space to the modal space. Equation (41) yields by left-multiplying of $\boldsymbol{\Phi}^T$ with the substitution of y:

$$\Phi^{\mathbf{T}}\mathbf{A}\Phi\dot{\mathbf{p}} + \Phi^{\mathbf{T}}\mathbf{B}\Phi\mathbf{p} = \Phi^{\mathbf{T}}\hat{\mathbf{f}} \quad (46)$$

The diagonal modal mass and stiffness matrix are

$$\boldsymbol{\Phi}^{\mathbf{T}}\mathbf{A}\boldsymbol{\Phi} = \begin{bmatrix} \ddots & & \\ & M_p & \\ & & \ddots \end{bmatrix}; \qquad \boldsymbol{\Phi}^{\mathbf{T}}\mathbf{B}\boldsymbol{\Phi} = \begin{bmatrix} \ddots & & \\ & K_p & \\ & & \ddots \end{bmatrix} \quad (47)$$

Then, rewrite Eq. (46) with the diagonal mass and stiffness matrices:

$$\begin{bmatrix} \ddots & & \\ & M_p & \\ & & \ddots \end{bmatrix}\dot{\mathbf{p}} + \begin{bmatrix} \ddots & & \\ & K_p & \\ & & \ddots \end{bmatrix}\mathbf{p} = \boldsymbol{\Phi}^{\mathbf{T}}\hat{\mathbf{f}} \quad (48)$$

Because of the relationship $\frac{\mathbf{K}_{\mathbf{p}i}}{\mathbf{M}_{\mathbf{p}i}} = -\lambda_i$, the previous equation converted to $2N$ numbers of the first-order linear ODE:

$$\dot{p}_i - \lambda_i p_i = \frac{1}{M_{pi}} \boldsymbol{\Psi}_{\mathbf{i}}^{\mathbf{T}} \hat{\mathbf{f}}_i \tag{49}$$

The steady-state solution of the previous equation when the system is at rest can be expressed as an integral equation and is also equivalent to the convolution in the time domain between the arbitrary force term $\frac{1}{M_{pi}} \Psi_i^T \hat{f}_i(t)$ and the dissipation term $e^{-\lambda_i t}$:

$$p_i = \frac{1}{M_{pi}} \int_0^t \boldsymbol{\Psi}_{\mathbf{i}}^{\mathbf{T}} \hat{\mathbf{f}}_{\mathbf{i}}(\boldsymbol{\tau}) \bullet e^{-\lambda_i (t-\tau)} \, \mathrm{d}\tau = \frac{1}{M_{pi}} \boldsymbol{\Psi}_{\mathbf{i}}^{\mathbf{T}} \hat{\mathbf{f}}_{\mathbf{i}}(\boldsymbol{t}) \otimes e^{-\lambda_i t} \tag{50}$$

Compared with the conventional integral method, the engineering value of this convolution method is easy to find. The conventional method requires the exact mathematical expression of this force in the time domain, yet the arbitrary force plot in the time domain is required by this convolution method. Thus, the modal superposition method can be established by

$$\mathbf{y} = \begin{Bmatrix} \mathbf{q} \\ \dot{\mathbf{q}} \end{Bmatrix} = \boldsymbol{\Phi} \mathbf{p} = \sum_{i=1}^{2N} \boldsymbol{\Psi}_{\mathbf{i}} p_i \tag{51}$$

Taking the curve-fitting range issue into consideration, it is necessary to sum up the modes only in the selected range, which has a lower number of modes than $2N$. In summary, the complex mode shape vector $\boldsymbol{\Psi}$ and the complex eigenvalue $\boldsymbol{\lambda}$ in each mode are key factors in determining the time-domain response for a viscoelastic damping structure.

VI. Results and Discussions

A. Comparison with Published Data for Different Boundary Conditions

In Fig. 6, a seven-layer sandwich beam with viscoelastic cores is shown, with the following design parameters listed in Table 2.

The previous data are used to predict the vibration performance of the system, using the numerical simulation method presented in this paper with the closed-form solution of Hao and Rao [2], as well as the simulation results from the commercial software ANSYS. In the ANSYS simulation, the two-dimensional element of plane 182 (four nodes) is selected, and the material damping effect is neglected. Thus, it can be expected that the natural frequency of each mode from the ANSYS results will be consistently higher than the result from considering the damping effect. As far as the curve-fitting result is concerned, the 3M ISD-110 at 45°C in Sec. IV is selected for the shear modulus of the viscoelastic layers in this numerical example. The different boundary conditions, including simply supported and clamp free, were investigated separately. The results are shown in Tables 3 and 4, respectively. It is seen that the agreement between the simulation presented in this paper, the closed-form solution, and the numerical result from ANSYS is very good for the simply-supported case. When the fixed-free boundary condition is applied, the simulation result presented in this paper also follows the identical trend compared with the ANSYS simulation result. This validates the analysis methodology proposed in the paper.

B. Vibration Performance with a Combination of Several Viscoelastic Materials at Different Temperatures

An important factor affecting the dynamic properties system with viscoelastic damping is the temperature. With an increase in temperature, the loss factor approaches its best performance toward the transition region and then decreases afterward. In this example, the 3M ISD-110 has a better damping performance than the 3M ISD-112 over the chosen temperature between 40 and 60°C. It is of interest to study the effect of the combination of these two viscoelastic materials on the damping structure.

To introduce the different viscoelastic materials, the seven-layer sandwich beam with the same parameters, as in the previous example, incorporating two damping materials (3M ISD-110 and 3M ISD-112) is designed. This system is compared with the same structure, with only one damping material (either the 3M ISD-110 or the 3M ISD-112). In the system, including the two viscoelastic materials, the outer damping layers (second and sixth) are the 3M ISD-112 and the inner damping layer (fifth) is the 3M ISD-110. Two different scenarios of boundary conditions are examined in this numerical example, and the temperature range is from 40 to 60°C. Figures 7a and 7b show the first-order natural frequency and the system loss factor over the temperature range, with the simply-supported boundary condition applied to the FEM.

On the other hand, Figs. 8a and 8b show the first-order vibration performance, including the natural frequency and the loss factor for

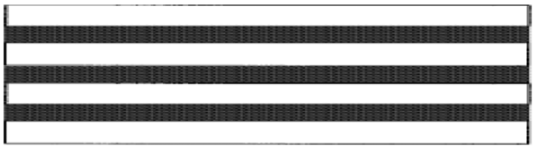

Fig. 6 Seven-layer sandwich structure with viscoelastic cores.

Table 2 Design parameters of seven-layer structure[a]

No. of layer	Height of layer	Elastic/viscoelastic properties	Material density
First	$h_1 = 1$ mm;	$E_1 = 210$ GPa	$\rho_1 = 7800$ kg/m^3
Second	$h_2 = 0.8$ mm;	G_2: Biot	$\rho_2 = 970$ kg/m^3
Third	$h_3 = 1$ mm;	$E_3 = 210$ GPa	$\rho_3 = 7800$ kg/m^3
Fourth	$h_4 = 0.8$ mm;	G_4: Biot	$\rho_4 = 970$ kg/m^3
Fifth	$h_5 = 1$ mm;	$E_5 = 210$ GPa	$\rho_5 = 7800$ kg/m^3
Sixth	$h_6 = 0.8$ mm;	G_6: Biot	$\rho_6 = 970$ kg/m^3
Seventh	$h_7 = 1$ mm;	$E_7 = 210$ GPa	$\rho_7 = 7800$ kg/m^3

[a]Length: 1 m, thickness: 0.1 m, number of elements: 12, and number of nodes: 13

Table 3 Comparison of results for simply-supported boundary condition

		ANSYS	Hao and Rao [2]	FEM of this paper
No. of Mode	Damping model	No damping	3M ISD-110 at 45°C Arrhenius	3M ISD-110 at 45°C six terms Biot
First	Frequency	6.037 Hz	4.7443 Hz	4.5834 Hz
	Loss factor	——	0.6248	0.7916
Second	Frequency	15.764 Hz	13.902 Hz	13.9489 Hz
	Loss factor	——	0.6008	0.6824
Third	Frequency	30.103 Hz	27.661 Hz	27.7721 Hz
	Loss factor	——	0.5317	0.5632
Fourth	Frequency	49.611 Hz	46.1548 Hz	47.1053 Hz
	Loss factor	——	0.4715	0.4681
Fifth	Frequency	74.434 Hz	69.3118 Hz	68.82259 Hz
	Loss factor	——	0.421	0.4226

Table 4 Comparison of results for fixed-free boundary condition

		ANSYS	FEM of this paper
No. of Mode	Damping model	No damping	ZN1 four terms Biot [18]
First	Frequency	3.5343 Hz	2.8453 Hz
	Loss factor	——	0.2351
Second	Frequency	11.885 Hz	11.35425 Hz
	Loss factor	——	0.4011
Third	Frequency	25.604 Hz	24.2774 Hz
	Loss factor	——	0.4969
Fourth	Frequency	44.635 Hz	40.756 Hz
	Loss factor	——	0.5268
Fifth	Frequency	68.813 Hz	62.4374 Hz
	Loss factor	——	0.5172

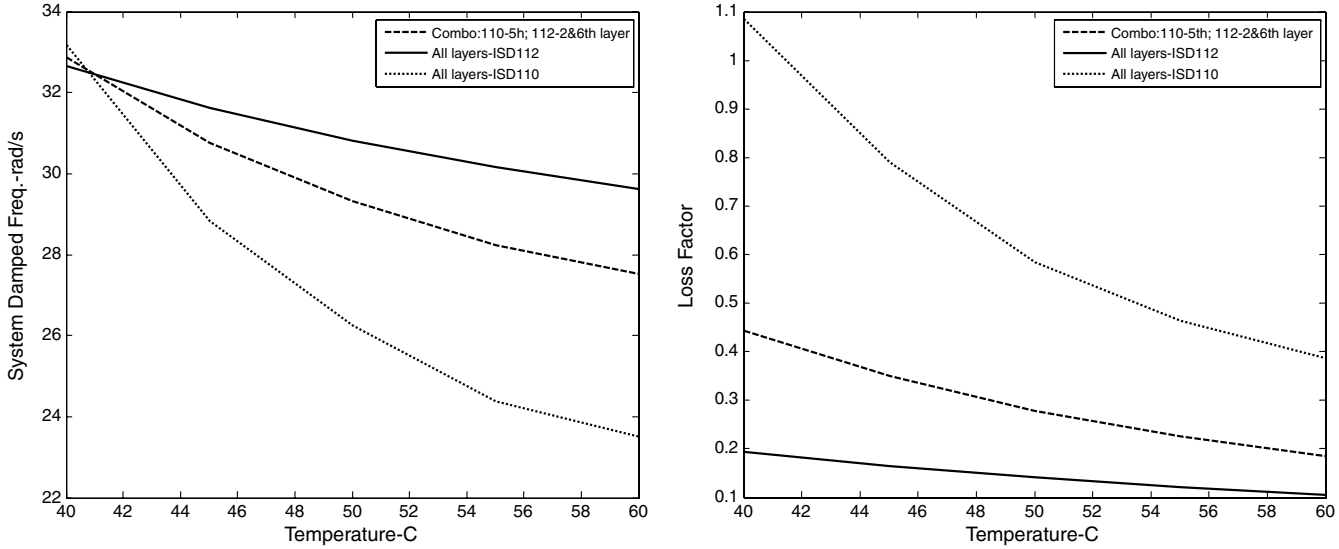

a) b)

Fig. 7 First system damped frequency/loss factor (simply-supported boundary condition).

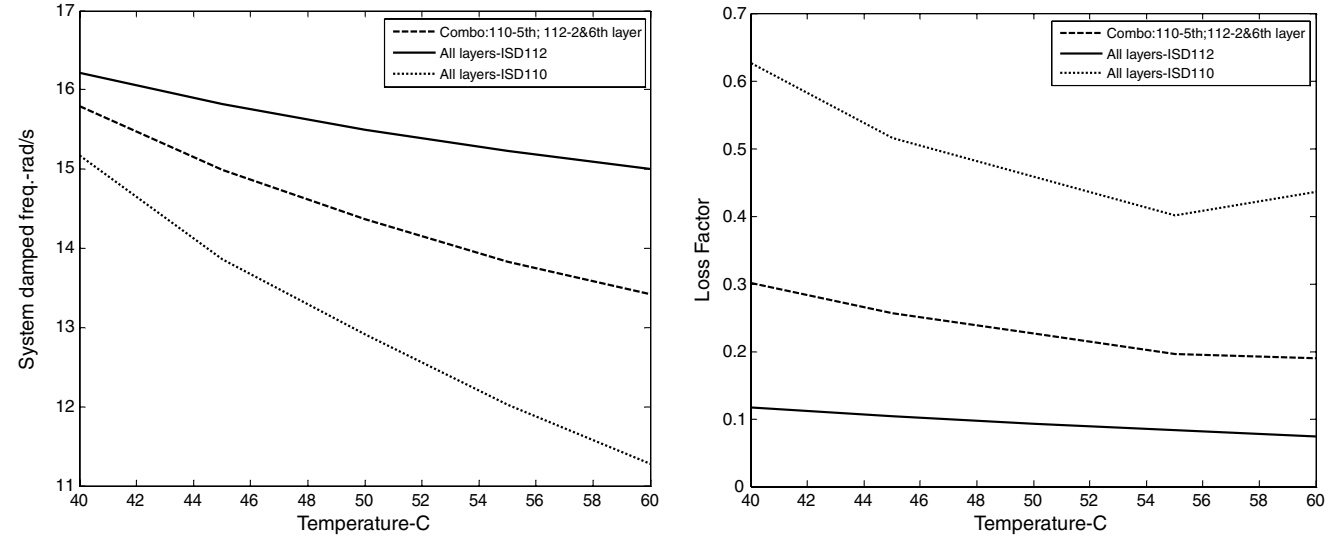

a) b)

Fig. 8 First damped frequency and loss factor of the system (fixed-free boundary condition).

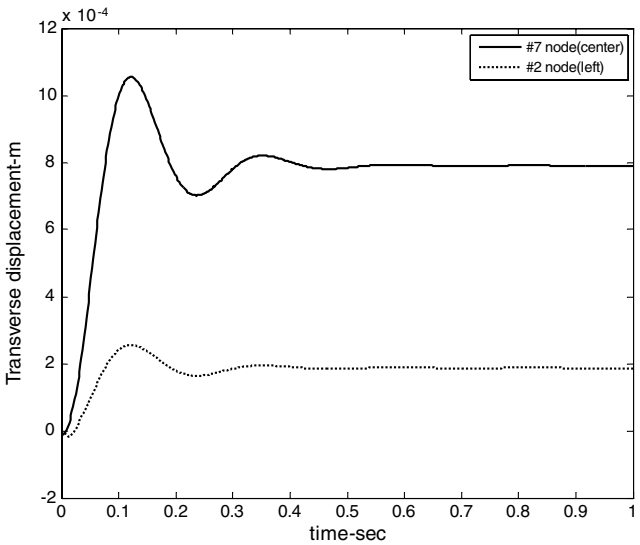

Fig. 9 System displacements under the unit step excitation.

the fixed-free boundary condition applied on this seven-layer structure. Comparing the loss factor of the first flexible mode of the simply-supported system, the same structure with the fixed-free boundary condition has less system damping at the corresponding temperature. It can be explained that the simply-supported boundary condition definitely has the advantage when it comes to maximum usage of the shear strain energy in the viscoelastic damping layer.

C. Time-Domain Response Under the Arbitrary Input

The plot in Fig. 9 shows the transverse displacement of two nodes (2 and 7) with a unit step force vertically applied on the middle not (7) of the simply-supported seven-layer sandwich beam, with the same design parameters as the previous example. The curve-fitting result of the 3M ISD-110 at the ambient temperature of 45°C is used in this example. This explains the energy dissipation phenomena in the time domain when an arbitrary force is applied on the structure.

VII. Conclusions

This paper presents a comprehensive procedure for applying the Biot damping model to a structural FEM by introducing different

types of viscoelastic materials. Several conclusions for each step can be drawn from this research.

1. The FEM of the multiple-layered damping beam is established by proper coordinate transforming of the two fundamental elements: the elastic layer and the constrained damping layer. This philosophy can be extended from the sandwich beam to a more complicated damping structure without much effort.

2. The nonlinear curve-fitting technique accurately prepares the Biot constants for further vibration analysis. Results through the procedure of vibration analysis discussed in this paper show good agreement when compared with the closed-form solution from previous work and the ANSYS result. The Biot damping model is also capable of improving the structure damping performance by adding new features, such as different viscoelastic materials, the variation of ambient temperature, etc.

3. Decoupling transformation not only solves the eigenvalue-based vibration problem, but it also successfully explains the time-domain response of energy dissipation. Another application of decoupling transformation-frequency-response-function-based analysis will be presented in future publications.

Appendix

In this supplemental section, the experimental data are provided by the Arrhenius empirical equation, including the damping properties, such as the shear modulus and loss factor for the 3M ISD-110 and -112 viscoelastic polymers. These viscoelastic materials have a different sensitivity than the complex shear modulus, with the change of temperature and frequency. The universal form of the empirical equation is listed as follows, and the complex shear modulus is calculated through

$$G^*(\omega) = G_c(1 + j\eta) \tag{A1}$$

In the previous equation, the real part of the shear modulus G_c is given by

$$\log(G_c) = \log(ML) + \frac{2 \times \log(MROM/ML)}{1 + (FROM/ML)^N} \tag{A2}$$

The equation of the loss factor η is

$$\log(\eta) = \log(ETAFR) + \frac{C}{2}[(S_L + S_H)A + (S_L - S_H)(1 - \sqrt{1 + A^2})] \tag{A3}$$

where A is

$$A = \frac{1}{C}\log\left(\frac{fr}{FROL}\right) \tag{A4}$$

The reduced-frequency-considered Arrhenius temperature shifting factor is

$$\log(fr) = \log(f) - \frac{12(T - T_0)}{291.66 + T - T_0} \tag{A5}$$

In previous equations, fr was the reduced frequency shifted by the temperature effect (Hz), f was the considered frequency (Hz), T was the temperature (°C), and $FROM$, $MROM$, N, ML, $ETAFROL$, S_L, S_H, $FROL$, C, and T_0 were the coefficients obtained, from the data sheet in Table A1, for the different type of viscoelastic materials.

Acknowledgments

We would like to thank Kaiyu Xu of Shanghai University, the People's Republic of China, for the helpful discussion on the FE modeling of the multiple-layered sandwich beam and his encouragement on this research.

References

[1] Mead, D. J., and Markus, S., "The Forced Vibration of a Three-Layer, Damped Sandwich Beam with Arbitrary Boundary Conditions," *Journal of Vibration and Acoustics*, Vol. 10, No. 2, 1969, pp. 163–175. doi:10.1016/0022-460X(69)90193-X

[2] Hao, M., and Rao, M. D., "Vibration and Damping Analysis of a Sandwich Beam Constraining a Viscoelastic Constraining Layer," *Journal of Composite Materials*, Vol. 39, No. 18, 2005 , pp. 1621–1643. doi:10.1177/0021998305051124

[3] Ungar, E. E., and Kerwin, E. M., "Loss Factors of Viscoelastic Systems in Terms of Energy Concepts," *Journal of the Acoustical Society of America*, Vol. 34, No. 7, 1962, pp. 954–957.

[4] Johnson, C., Keinholz, D., and Rongers, L., "Finite Element Prediction of Damping in Structures with Constrained Viscoelastic Layers," *AIAA Journal*, Vol. 20, No. 9, 1982, pp. 1284–1290. doi:10.2514/3.51190

[5] Bagley, R. L., "Fractional Calculus: a Different Approach to the Analysis of Viscoelastic Damped Structure," *AIAA Journal*, Vol 21 No. 5, 1983, pp. 741–748. doi:10.2514/3.8142

[6] Lesieutre, G. A., and Bianchini, E., "Finite Element Method of One-Dimensional Viscoelastic Structures Using Anelastic Displacement Fields," *Journal of Guidance, Control, and Dynamics*, Vol. 19, No. 3, May–June 1996, pp. 520–527. doi:10.2514/3.21652

[7] Lesieutre, G. A., and Lee, U., "A Finite Element For Beams Having Segmented Active Constrained Layers With Frequency," *Smart Materials and Structures*, Vol. 5 Oct. 1996, pp. 615–627. doi:10.1088/0964-1726/5/5/010

[8] Biot, M. A., "Variational Principles in Irreversible Thermodynamic with Application to Viscoelasticity," *Physical Review*, Vol. 97, No. 6, 1955, pp. 1463–1469. doi:10.1103/PhysRev.97.1463

[9] McTavish, D. J., "Shock Response of a Damped Linear Structure Using GHM Finite Elements," AIAA Paper 2003-1591, April 2003.

[10] Yiu, Y. C., "Finite Element Analysis of Structures with Classical Viscoelastic Materials," 34th AIAA/ASME/ASCE/AHS/ASC Structures, Structural Dynamics, and Materials Conference, AIAA Paper 1993-1551, April 1993.

[11] Adhikari, S., "Damping Models for Structural Vibration," Ph.D. Thesis, Engineering Dept., Cambridge Univ., Cambridge, England, U.K., Sept. 2000.

[12] Rao, M. D., "Recent Applications of Viscoelastic Damping for Noise Control in Automobiles and Commercial Airplanes," *Journal of Sound and Vibration*, Vol. 262, No. 3, 2003, pp. 457–474. doi:10.1016/S0022-460X(03)00106-8

[13] Plass, H. J., "Damping of Vibrations in Elastic Rods and Sandwich Structures by Incorporation of Additional Viscoelastic Material," *3rd Midwestern Conference on Solid Mechanics*, 1957, pp. 48–71.

[14] Kerwin, E. M., "Damping of Flexural Waves by a Constrained Viscoelastic Layer," *Journal of the Acoustical Society of America* Vol. 31, No. 7, 1959, pp. 952–962. doi:10.1121/1.1907821

[15] DiTaranto, R. A., "Theory of Vibratory Bending for Elastic and Viscoelastic Layered Finite-Length Beams," *Journal of Applied Mechanics*, Vol. 32, Dec. 1965, pp. 881–886.

[16] Ma, B. A., "Loss Factor and Natural Frequency of Five-Layer Viscoelastic Damping Beam," *Journal of Applied Mechanics*, Feb 1980, pp. 39–43 (in Chinese).

[17] Hao, M., and Rao, M. D., "Optimum Design of Multiple-Constraint Layered Systems for Vibration Control," *AIAA Journal*, Vol. 42, No. 12,

Table A1 Arrhenius coefficients from [20]

			Modulus parameters				Loss factor parameters				
Damping material	Density, kg/m^3	T_0, c	$FROM$	$MROM$, N/m^2	N	ML, N/m^2	$ETAFR$	S_L	S_H	$FROL$	C
3M ISD-110	970	70	5e − 3	2e − 6	0.35	5.5e − 4	1.3	0.35	−0.4	2e − 3	2
3M ISD-112	970	55	4e − 5	1.61e − 7	0.276	1.72e − 5	1.25	0.27	−0.35	1.503 − 5	1.3

Dec. 2004, pp. 2448–2461.
doi:10.2514/1.1964

[18] Zhang, J., Zheng, G. T., and Huang, W. H., "The Biot Model and Its Application in Viscoelastic Composite Structures," *Journal of Vibration and Acoustics*, Vol. 129, No. 5, Oct. 2007, pp. 533–541.
doi:10.1115/1.2731408

[19] Chandrupatla, T. R., and Belegundu, A. D., *Introduction to Finite Elements in Engineering*, 3rd ed., Prentice–Hall, Upper Saddle River, NJ, Jan 2002.

[20] Hao, M., "Vibration Analysis of Constrained Layered Beams with Multiple Damping Layers," Ph.D. Dissertation, MEEM Dep., Michigan Technological Univ., Houghton, MI, May 2005.

J. Wei
Associate Editor